

# Dynamic Buckling of Conical Shells with Imperfections

A. C. SHIAU\*

*State University of New York at Buffalo, Buffalo, N.Y.*

AND

R. S. ROTH†

*AVCO Corporation, Wilmington, Mass.*

AND

T. T. SOONG‡

*State University of New York at Buffalo, Buffalo, N.Y.*

A study has been made to determine the dynamic stability of a truncated thin circular conical shell with various geometrical imperfections and under a wide variety of dynamic loading conditions. The method of solutions utilizes a Galerkin procedure. By assuming the deformation modes, the final nonlinear differential equations of motion are derived by minimizing the total energy of the system with respect to each of the undetermined modal amplitudes. A Runge-Kutta integration scheme is then used to solve these nonlinear differential equations numerically. From the characteristics of the shell response, a criterion for the buckling load is established. It is found that the tendency of dynamic buckling of a conical shell structure decreases with increase of the opening angle of the cone. Conical shells are also found to be less sensitive to initial geometric imperfections than the cylinder.

## I. Introduction

SINCE the early investigation by Donnell,<sup>1</sup> the dynamic response of shell structures has been the subject of numerous studies over the past decade. More recently, important imperfection—sensitive characteristics of shells have been investigated by many authors.<sup>2-8</sup> However, most of the efforts in this direction have been confined to the cylindrical shell problem. It is the purpose of this paper to investigate the dynamic response of a truncated conical shell structure with various initial imperfections under a suddenly applied axial edge load and a uniform lateral hydrostatic pressure.

Thin shells in the form of circular conical frustums are closely related to the cylindrical shells geometrically: the conical shell simply reduces to a cylindrical shell when the semivertex angle of the cone becomes zero and the minimum radius of curvature of the median surface approaches a constant value. Similarly, it reduces to a flat circular plate when the semivertex angle of the cone approaches a right angle. Therefore, a single analysis can be used to study these three closely related problems.

The general analytical solutions for some elastic cone problems are discussed in some detail by Love in his treatise,<sup>9</sup> where rigorous equations governing the deformations of middle surface of the shell are established. On the problem of asymmetrical bending of conical shells under arbitrary loads, a set of equations which reduces to Donnell's equations for circular cylindrical shells in the limit was presented first by Hoff<sup>10</sup> and was later modified by Seide.<sup>11</sup> However, both Hoff and Seide are primarily concerned with the derivation of the shell equations and boundary conditions, and it appears that relatively little progress has been made in finding solutions from which numerical results can be obtained. Furthermore, when the initial imperfections are

introduced it is in general difficult to derive a set of Karman-Donnell type equations for a cone, because a satisfactory stress function is not always obtainable. Therefore, rather than attempt to derive such equations for the cone, we will use an energy approach by which numerical solutions may be carried out for dynamic response of the shell.

The technique of solution utilizes a Galerkin procedure in which deformations are assumed to be linear combinations of chosen mode shapes. Each mode shape is multiplied by an unknown and time-dependent amplitude. The initial imperfections are likewise assumed. Based on Seide's work, the middle-surface strain-displacement relationships and the expressions for curvatures of a deformed thin conical shell with small initial imperfections are derived. The total energy function of the system is then expressed in terms of initial imperfections. A set of nonlinear differential equations of motion are found by minimizing the total energy of the system with respect to each of the unknown amplitudes representing responses of the modes.

It is noted that the boundary conditions of the problem are reflected in a particular choice of the mode shapes, while the initial conditions are arbitrary. Final solutions of the governing equations of motion are found numerically by a Runge-Kutta integration scheme.

## II. Analytical Formulation

### A. Physical Problem

The physical problem considered in this study is to determine the dynamic response of a truncated thin circular conical shell structure, having initial imperfections and subject to both an arbitrary time-dependent axial edge load and a uniform hydrostatic pressure. The geometry of the system is defined in Fig. 1. We assume throughout the study that the shell is stressed elastically. A nonlinear large deflection shell theory is used to analyze the dynamic instability of the system.

### B. Middle-Surface Deformations and Stresses

Based upon Seide,<sup>11</sup> the middle-surface strain-displacement relationships and the modified expressions for curvatures of a deformed thin conical shell with slight initial imperfections are

Received September 13, 1973. This research was supported in part by the National Science Foundation under Grants GK-1834X and GK-31229.

Index categories: Structural Dynamic Analysis; Structural Stability Analysis.

\* Research Assistant, Faculty of Engineering and Applied Sciences; presently Research Engineer, Foster Wheeler Corporation, Livingston, N.J.

† Senior Staff Scientist, Systems Division.

‡ Professor, Faculty of Engineering and Applied Sciences.

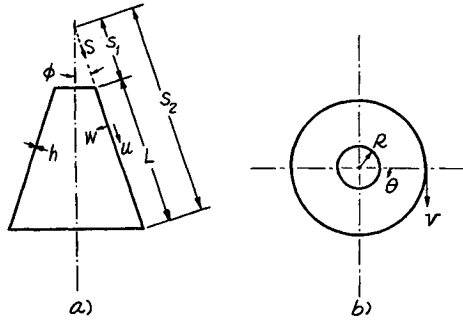


Fig. 1 Shell geometry.

$$\begin{aligned}
 \varepsilon_s &= u_{,s} + \frac{1}{2} w_{,s}^2 + w_{,s} \bar{w}_{,s} \\
 \varepsilon_\theta &= (u - w \cot \phi)/s + v_{,\theta}/(s \sin \phi) + \frac{1}{2} [w_{,\theta}/(s \sin \phi)]^2 + w_{,\theta} \bar{w}_{,\theta}/(s \sin \phi)^2 \\
 \gamma_{s\theta} &= v_{,s} - v/s + (u_{,\theta} + w_{,s} w_{,\theta} + w_{,s} \bar{w}_{,\theta} + w_{,\theta} \bar{w}_{,s})/(s \sin \phi) \\
 x_s &= w_{,ss} \\
 x_\theta &= w_{,s}/s + w_{,\theta\theta}/(s \sin \phi)^2 \\
 x_{s\theta} &= (w_{,s\theta}/s - w_{,\theta}/s^2)/\sin \phi
 \end{aligned} \quad (1)$$

where  $\bar{w}$  represents initial imperfections in the geometry and the comma denotes differentiation with respect to the spatial variables.

The axial, circumferential, and shear stresses in the middle surface are expressed in terms of the middle-surface strains by the usual form of Hooke's Law

$$\begin{aligned}
 \sigma_s &= (E/(1-\nu^2))(\varepsilon_s + \nu \varepsilon_\theta) \\
 \sigma_\theta &= (E/(1-\nu^2))(\varepsilon_\theta + \nu \varepsilon_s) \\
 \tau_{s\theta} &= \{E/[2(1+\nu)]\} \gamma_{s\theta}
 \end{aligned} \quad (2)$$

where  $\sigma_s$  and  $\sigma_\theta$  are positive in tension,  $E$  is the modulus of elasticity and  $\nu$  denotes Poisson's ratio.

Therefore, for a thin shell, the force and moment resultants are related to strains and curvatures by

$$\begin{aligned}
 N_s &= (Eh/(1-\nu^2))(\varepsilon_s + \nu \varepsilon_\theta) \\
 N_\theta &= (Eh/(1-\nu^2))(\varepsilon_\theta + \nu \varepsilon_s) \\
 N_{s\theta} &= N_{\theta s} = [Eh/2(1+\nu)] \gamma_{s\theta} \\
 M_s &= -D(x_s + \nu x_\theta) \\
 M_\theta &= -D(x_\theta + \nu x_s) \\
 M_{s\theta} &= -M_{\theta s} = D(1-\nu)x_{s\theta}
 \end{aligned} \quad (3)$$

where the bending stiffness is

$$D = Eh^3/12(1-\nu^2) \quad (4)$$

### C. Potential and Kinetic Energy

The potential energy is expressible as

$$U = V_1 + V_2 - V_3 - V_4 \quad (5)$$

with

$$V_1 = \int_0^{2\pi} \int_{s_1}^{s_2} \frac{1}{2} [N_s \varepsilon_s + N_\theta \varepsilon_\theta + N_{s\theta} \gamma_{s\theta}] s \sin \phi \, ds \, d\theta \quad (6)$$

$$V_2 = \int_0^{2\pi} \int_{s_1}^{s_2} \frac{1}{2} [-M_s x_s - M_\theta x_\theta + 2M_{s\theta} x_{s\theta}] s \sin \phi \, ds \, d\theta \quad (7)$$

$$V_3 = -\sigma h \int_0^{2\pi} [u(s_1, \theta) \cos \phi + w(s_1, \theta) \sin \phi] s_1 \sin \phi \, d\theta \quad (8)$$

$$V_4 = -q \int_0^{2\pi} \int_{s_1}^{s_2} w s \sin \phi \, ds \, d\theta \quad (9)$$

where the axial edge stress  $\sigma$  and the pressure  $q$  are positive in tension.

The quantities  $V_1$  and  $V_2$  can be expressed in terms of displacements by substituting the proper relationships given in Eqs. (1) and (3) into Eqs. (6) and (7).

The kinetic energy is

$$T = \frac{1}{2} \rho h \int_0^{2\pi} \int_{s_1}^{s_2} \left[ \left( \frac{\partial u}{\partial t} \right)^2 + \left( \frac{\partial v}{\partial t} \right)^2 + \left( \frac{\partial w}{\partial t} \right)^2 \right] s \sin \phi \, ds \, d\theta \quad (10)$$

where  $\rho$  is the material density and  $t$  denotes time.

### D. Coordinate Transformations and Nondimensional Parameters

The energy functions can be simplified by introducing the following change of coordinates

$$s = s_1 e^x, \quad y = \theta \sin \phi \quad (11)$$

We then have

$$V_1 = Ehs_1^2/[2(1-\nu^2)] \int_0^{x_0} \int_0^{y_0} \{ e^{2x} [(\varepsilon_x + \varepsilon_y)^2 - 2(1-\nu)\varepsilon_x \varepsilon_y + \frac{1}{2}(1-\nu)\gamma_{xy}^2] \} dx \, dy \quad (12a)$$

$$V_2 = \frac{1}{2} Ds_1^2 \int_0^{x_0} \int_0^{y_0} \{ e^{2x} [(\nabla^2 w)^2 - 2(1-\nu)/(s_1 e^x)^4 \{ (w_{,xx} - w_{,x}][w_{,x} + w_{,yy}] - [w_{,xy} - w_{,y}]^2 \} ] \} dx \, dy \quad (12b)$$

where

$$\nabla^2 w = (w_{,xx} + w_{,yy})/s_1^2 e^{2x}$$

and

$$V_3 = -\sigma h s_1 \int_0^{y_0} [u(0, y) \cos \phi + w(0, y) \sin \phi] dy \quad (12c)$$

$$V_4 = -q s_1^2 \int_0^{x_0} \int_0^{y_0} e^{2x} w \, dx \, dy \quad (12d)$$

$$T = \frac{1}{2} \rho h s_1^2 \int_0^{x_0} \int_0^{y_0} e^{2x} \left[ \left( \frac{\partial u}{\partial t} \right)^2 + \left( \frac{\partial v}{\partial t} \right)^2 + \left( \frac{\partial w}{\partial t} \right)^2 \right] dx \, dy \quad (12e)$$

In the preceding equations, the upper limits of the integrals are defined by

$$x_0 = \ln(s_2/s_1), \quad y_0 = 2\pi \sin \phi \quad (13)$$

The strains, written in the new coordinate system, are

$$\begin{aligned}
 \varepsilon_x &= (1/s_1 e^x) [u_{,x} + (\frac{1}{2} w_{,x}^2 + w_{,x} \bar{w}_{,x})/s_1 e^x] \\
 \varepsilon_y &= (1/s_1 e^x) [u - w \cot \phi + v_{,y} + (\frac{1}{2} w_{,y}^2 + w_{,y} \bar{w}_{,y})/s_1 e^x] \\
 \gamma_{xy} &= (1/s_1 e^x) [v_{,x} - v + u_{,y} + (w_{,x} w_{,y} + w_{,x} \bar{w}_{,y} + w_{,y} \bar{w}_{,x})/s_1 e^x]
 \end{aligned} \quad (14)$$

As was mentioned before, a cylinder problem can be considered as a limiting case of the cone problem. A brief examination of the formulation shows that the governing equations of the cylinder can be recovered from those of the cone through the limiting processes  $s_1 \rightarrow \infty$  and  $\phi \rightarrow 0$  with  $s_1 \sin \phi = R$ . However, these limits imply that  $x_0 \rightarrow 0$  and  $y_0 \rightarrow 0$ , so that in the limit the energy expressions are not easily defined. Therefore, it is necessary to apply a second transformation to the system in order to approach the limit properly. Hence, let

$$\xi = x/x_0, \quad \eta = y/y_0 \quad (15)$$

and introduce the parameters

$$\begin{aligned}
 \alpha &= h/R & \bar{\sigma} &= -\sigma R/Eh \\
 \beta &= R/L & \bar{q} &= -qR/Eh \\
 \bar{\alpha} &= s_1 x_0/L & \bar{w}^* &= \bar{w}/h
 \end{aligned} \quad (16)$$

Then, if the displacements are nondimensionalized by the thickness  $h$ , i.e.,  $w^* = w/h$ , etc., and a nondimensional time  $\tau$  is introduced by the relation

$$\tau = ct/R, \quad c = (E/\rho)^{1/2} \quad (17)$$

we have

$$\begin{aligned}
 \varepsilon_\xi &= e^{-x_0 \xi} [(\alpha \beta / \bar{\alpha}) u_{,\xi}^* + (\alpha \beta / \bar{\alpha})^2 e^{-x_0 \xi} (\frac{1}{2} w_{,\xi}^{*2} + w_{,\xi}^* \bar{w}_{,\xi}^*)] \\
 \varepsilon_\eta &= e^{-x_0 \xi} [\alpha (u^* \sin \phi - w^* \cos \phi) + (\alpha/2\pi) v_{,\eta}^* + (1/4\pi^2) \alpha^2 e^{-x_0 \xi} (\frac{1}{2} w_{,\eta}^{*2} + w_{,\eta}^* \bar{w}_{,\eta}^*)] \\
 \gamma_{\xi\eta} &= e^{-x_0 \xi} [(\alpha \beta / \bar{\alpha}) v_{,\xi}^* - \alpha \sin \phi v^* + (\alpha/2\pi) u_{,\eta}^* + (1/2\pi) (\alpha^2 \beta / \bar{\alpha}) e^{-x_0 \xi} (w_{,\xi}^* w_{,\eta}^* + w_{,\xi}^* \bar{w}_{,\eta}^* + w_{,\eta}^* \bar{w}_{,\xi}^*)]
 \end{aligned} \quad (18)$$

and

$$V_1 = (\pi E h^3 L / R) \left\{ \bar{\alpha} / [\alpha^2 (1 - \nu^2)] \int_0^1 \int_0^1 e^{2x_0 \xi} [(\epsilon_\xi + \epsilon_\eta)^2 - 2(1 - \nu) \epsilon_\xi \epsilon_\eta + \frac{1}{2}(1 - \nu) \gamma_{\xi\eta}^2] d\xi d\eta \right\} \quad (19a)$$

$$V_2 = (\pi E h^3 L / R) \left\{ \bar{\alpha} / [12\alpha^2 (1 - \nu^2)] \int_0^1 \int_0^1 e^{2x_0 \xi} \{ [(\alpha\beta/\bar{\alpha})^2 w_{,\xi\xi}^* + (\alpha/2\pi)^2 w_{,\eta\eta}^*]^2 - 2(1 - \nu) [(\alpha\beta/\bar{\alpha})^2 (w_{,\xi\xi}^* - x_0 w_{,\xi}^*) \times [x_0 (\alpha\beta/\bar{\alpha})^2 w_{,\xi\xi}^* + (\alpha/2\pi)^2 w_{,\eta\eta}^*] - \{ [\alpha^2 \beta / 2\pi \bar{\alpha}] (w_{,\xi\eta}^* - x_0 w_{,\eta}^*)^2 \}] \} d\xi d\eta \right\} \quad (19b)$$

$$V_3 = (\pi E h^3 L / R) \left\{ 2\bar{\sigma} \beta \left( \int_0^1 [u^*(0, \eta) \cos \phi + w^*(0, \eta) \sin \phi] d\eta \right) \right\} \quad (19c)$$

$$V_4 = (\pi E h^3 L / R) \left[ 2q(\bar{\alpha}/\alpha) \int_0^1 \int_0^1 e^{2x_0 \xi} w^* d\xi d\eta \right] \quad (19d)$$

$$T = (\pi E h^3 L / R) \left[ \bar{\alpha} \int_0^1 \int_0^1 e^{2x_0 \xi} (\dot{u}^{*2} + \dot{v}^{*2} + \dot{w}^{*2}) d\xi d\eta \right] \quad (19e)$$

where

$$(\dot{\phantom{x}}) = (\partial/\partial\tau)(\phantom{x}) \quad (20)$$

#### E. Deformation Functions

The object of this study is to solve the response problem when specific functional forms of the displacements and the initial imperfections are chosen. Let the deformation functions and the initial imperfections take the following form:

$$\begin{aligned} u &= h[u_2(\tau)f_1(n\pi\xi)\sin m\pi\eta + u_1(\tau)(\bar{\alpha}/\alpha\beta)(\xi - 1)] \\ v &= h[v_2(\tau)f_2(n\pi\xi)\cos m\pi\eta] \\ w &= h[w_3(\tau)f_3(n\pi\xi)\sin m\pi\eta + w_2(\tau)f_4(2n\pi\xi) + w_1(\tau)] \\ \bar{w} &= h[d_1 f_5(n\pi\xi)\sin m\pi\eta] \end{aligned} \quad (21)$$

The boundary conditions implied by the abovementioned deformation functions are that the shell is free at the top and restrained from moving in the  $u$ -direction at the bottom. A uniform breathing mode in  $w$  is allowed, so  $w$  is not restrained at the ends. The slope of  $w$  is zero, however, thus preventing any rotation at the ends. The symmetric mode of deformation of the shell is allowed by the uniform compression  $u_1$  and the breathing mode  $w_1$ . The buckling modes thus are included in the terms  $u_2$ ,  $v_2$ ,  $w_2$ , and  $w_3$ . The tangential deformation is zero at both ends of the shell, whose action will tend to stiffen the shell.

#### F. Hamilton's Principle and the Equations of Motion

Hamilton's Principle states that the actual motion of a system whose Lagrangian is

$$\bar{L}(u, v, w; \dot{u}, \dot{v}, \dot{w}) = T - (V_1 + V_2 - V_3 - V_4) \quad (22)$$

is such as to render the integral

$$I = \int_{t_1}^{t_2} \bar{L} dt \quad (23)$$

an extremum with respect to the displacements  $u$ ,  $v$ , and  $w$ . The Euler-Lagrange equations are

$$\frac{\partial \bar{L}}{\partial z_i} - \frac{d}{dt} \left( \frac{\partial \bar{L}}{\partial \dot{z}_i} \right) = 0, \quad i = 1, 2, \dots, 6 \quad (24)$$

where

$$(z_1, \dots, z_6) = (u_1, u_2, v_2, w_1, w_2, w_3) \quad (25)$$

Therefore, if the total energy is minimized with respect to each of the unknown amplitudes by substituting the proper energies

into the Euler-Lagrange equations of motion, the final nonlinear differential equations of motion for the dynamic response of an elastic conical shell become

$$\ddot{u}_1 + a_1 u_1 + a_2 w_2 + a_3 w_1 + a_4 w_2^2 + a_5 w_3^2 + a_6 w_3 d_1 = a_7 \bar{\sigma} \quad (26a)$$

$$\ddot{u}_2 + a_8 u_2 + a_9 w_2 w_3 + a_{10} w_2 d_1 + a_{11} w_3 + a_{12} v_2 = 0 \quad (26b)$$

$$\ddot{v}_2 + a_{13} v_2 + a_{14} u_2 + a_{15} w_3 + a_{16} w_2 w_3 + a_{17} w_2 d_1 = 0 \quad (26c)$$

$$\begin{aligned} \ddot{w}_3 + (a_{18} + a_{19} u_1 + a_{20} w_1 + a_{21} w_2 + a_{22} w_3^2 + a_{23} w_2^2 + a_{24} d_1^2 + \\ a_{25} w_3 d_1) w_3 + a_{26} u_2 w_2 + a_{27} v_2 + a_{28} w_2^2 d_1 + a_{29} u_1 d_1 + \\ a_{30} w_2 d_1 + a_{31} w_1 d_1 + a_{32} v_2 w_2 + a_{33} u_2 = 0 \end{aligned} \quad (26d)$$

$$\begin{aligned} \ddot{w}_2 + a_{34} \ddot{w}_1 + (a_{35} + a_{36} u_1 + a_{37} w_1 + a_{38} d_1^2 + a_{39} w_2^2 + \\ a_{40} w_3^2 + a_{41} w_3 d_1 + a_{42} w_2) w_2 + a_{43} u_2 w_3 + a_{44} u_2 d_1 + \\ a_{45} u_1 + a_{46} w_3^2 + a_{47} w_3 d_1 + a_{48} v_2 d_1 + a_{49} w_1 + \end{aligned}$$

$$a_{50} v_2 w_3 = a_{51} \bar{\sigma} + a_{52} \bar{q} \quad (26e)$$

$$\ddot{w}_1 + a_{53} \ddot{w}_2 + a_{54} w_1 + a_{55} u_1 + a_{56} w_2 + a_{57} w_2^2 + a_{58} w_3^2 +$$

$$a_{59} w_3 d_1 = a_{60} \bar{\sigma} + a_{61} \bar{q} \quad (26f)$$

The coefficients  $a_1$  through  $a_{61}$  in the equations of motion are lengthy and complicated and, in order to save space, they are not documented here. These coefficients can be found in Ref. 14.

### III. Criterion for Dynamic Buckling Load

One definition of the dynamic buckling load has been given by Budiansky and Roth<sup>12</sup> to be the load at which a large increase in amplitudes of the deflections occurs. The solutions of the system of equations of motion (26) can therefore be used to determine the critical buckling load. Qualitatively, if the time histories of the modes of the deformations are given for several levels of a constantly applied load, the critical buckling load can simply be identified as the load at which a large increase in the amplitudes of the deformations is seen to occur.

In a more quantitative manner, another buckling criterion can be established which is similar to that used by Roth and Klosner.<sup>5</sup> Consider responses of the deformation modes. Previous numerical results have shown that, as the load  $\bar{\sigma}$  increases, the time to a significant maximum increases until a certain load is reached. After this load is reached, however, the time to such a maximum decreases. If the magnitude of this maximum of the mode is plotted against the applied load, it can be observed that, associated with the reversal in the time trend to this maximum, the magnitude of the mode takes a sudden jump in value. That is, at this load, the behavior of the structure changes radically, indicating instability. Thus, an instability criterion is established by investigating the times to first maxima in the responses of the modes of deformations. The load at which a reversal in the time to first maximum occurs is defined to be the critical load.

Among the six modes of deformations in Eqs. (21), however, only  $u_2$ ,  $v_2$ ,  $w_2$ , and  $w_3$  represent the buckling modes, while  $u_1$  gives a uniform compression, and  $w_1$  is simply a symmetric breathing mode. Therefore what needs to be investigated in determining a buckling load are only those responses included in the buckling modes.

As a rule, since the  $w_2$  mode has played a dominant role in our investigation, the buckling load will be determined by simply investigating the response of the  $w_2$  mode only. In the following calculations, the critical loads are identified using the time reversal criterion with respect to the  $w_2$  mode. As will be seen, jumps in deformation are always present at this load.

### IV. Numerical Results

#### A. Perfect Cylindrical Shells

Considered first is the dynamic buckling of a perfect cylindrical shell under a suddenly applied axial load of constant magnitude and prolonged time duration. This example is chosen to demonstrate the validity of the analysis by finding the critical axial

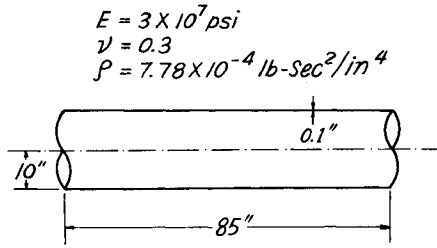


Fig. 2 Cylindrical shell.

buckling load of a perfect cylinder, and comparing it with known results. The geometry of the shell under study is shown in Fig. 2.

The deformation functions are assumed to have the following form:

$$\begin{aligned} u &= h[u_2(\tau) \sin n\pi\xi(1 - \cos n\pi\xi) \sin m\pi\eta + u_1(\tau)(\bar{\alpha}/\alpha\beta)(\xi - 1)] \\ v &= h[v_2(\tau) \sin n\pi\xi \cos m\pi\eta] \end{aligned} \quad (27)$$

$$w = h[w_3(\tau) \cos n\pi\xi \sin m\pi\eta + w_2(\tau) \cos 2n\pi\xi + w_1(\tau)]$$

and  $\bar{w} = 0$ , since the shell is assumed to be a perfect cylinder.

For  $m = 6$  and  $n = 30$ , the response of the  $w_2$  mode is shown in Fig. 3 for several nondimensional axial load levels. A plot of the maximum response of the  $w_2$  mode vs the load level is shown in Fig. 4 which is useful for determining the critical dynamic buckling load.

It can be seen clearly in Fig. 3 that the response of the  $w_2$  mode is uniformly very small for a load parameter value under 0.6. At a load parameter value of 0.6 and above, the response becomes significantly higher. Thus dynamic instability is clearly present and is initiated earlier for each increased load parameter. An examination of Fig. 4 also indicates that dynamic instability has occurred at a load parameter value  $\bar{\sigma} = 0.6$ . This is exactly the critical load found by Kempner<sup>13</sup> and others for the linear eigenvalue problem and by Roth and Klosner<sup>5</sup> for the dynamic case.

### B. Cylindrical Shells with Initial Imperfections

This problem is similar to case A except that an initial imperfection in the  $w$ -direction is introduced. It is assumed that the shell has an initial imperfection described by

$$\bar{w} = h(d_1 \cos n\pi\xi \sin m\pi\eta) \quad (28)$$

where  $d_1$  is a known nondimensional parameter of the imperfection amplitude.

Figure 5 shows the dynamic response of the  $w_2$  mode for  $d_1 = 0.1$ . The critical buckling load is found to be  $\bar{\sigma} = 0.45$ . Similarly, for  $d_1 = 0.5$ , a critical load is 0.4. These results are also in agreement with those obtained by Roth and Klosner<sup>5</sup> provided that the imperfections are small.

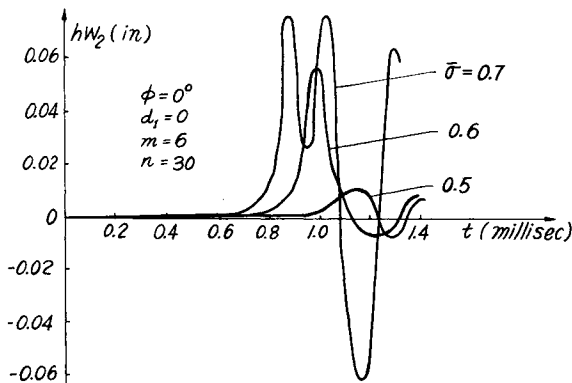


Fig. 3 The  $w_2$  mode vs time for various load parameter  $\bar{\sigma}$ .

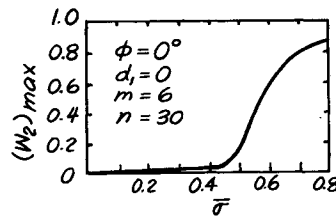


Fig. 4 Variation of maxima of  $w_2$  mode with load parameter  $\bar{\sigma}$ .

Comparing these results with that of the previous example, it is seen that the axial load-carrying capacity of a cylindrical shell is greatly reduced by the presence of initial imperfections. This imperfection-sensitive property of cylindrical shells has been observed by many other authors.<sup>3-8</sup>

### C. Conical Shells

The dynamic buckling of thin circular conical shells under a suddenly applied axial load, with or without initial imperfections, is considered next. This is carried out for several values of the opening angle  $\phi$  with the following dimensions:

$$h = 0.1 \text{ in.}, \quad R = 10 \text{ in.}, \quad L \cos \phi = 85 \text{ in.}$$

Similar to the cylindrical shell case, the periodic vibration of the time histories in the  $u_1$  mode evaluated at the top of the conical shell does not give clear indications of the onset of buckling. A study of the numerical results also shows that the  $u_2$  and  $v_2$  modes are generally small in comparison with the normal deflection mode. Moreover, the response of the  $w_3$  mode and the breathing mode  $w_1$  illustrate similar nonlinear behavior as that of the  $w_2$  mode. Thus, for a thin axial-loaded circular

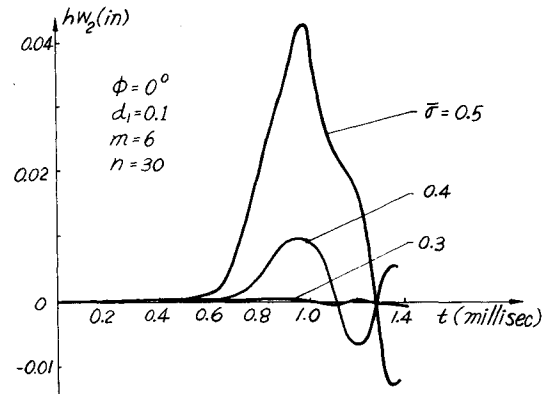


Fig. 5 Cylindrical shell with initial imperfection.

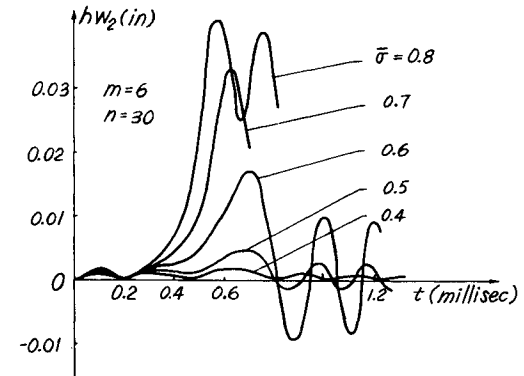


Fig. 6 Conical shell ( $\phi = 15^\circ$  and  $d_1 = 0$ ).

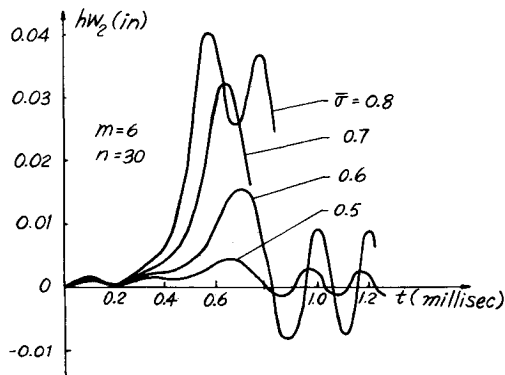


Fig. 7 Conical shell ( $\phi = 15^\circ$  and  $d_1 = 0.1$ ).

conical shell, the instability criterion of investigating the response of only the  $w_2$  mode is justified.

The results of the dynamic response of the  $w_2$  mode for a conical shell are presented in Figs. 6–11, each associated with a set of initial imperfection and opening angle of the shell. The critical load for each case is summarized in Table 1.

The results show that a conical shell structure is not as sensitive to its geometric imperfections as in the case of a cylindrical shell. The buckling load increases with the increase of the opening angle. The axial load-carrying capacity of a conical shell is thus improved by increasing the opening angle of the cone.

However, we note that, although extending the opening angle tends to stabilize the structure, the boundary conditions need to be examined carefully. Less judicious choice of deformation

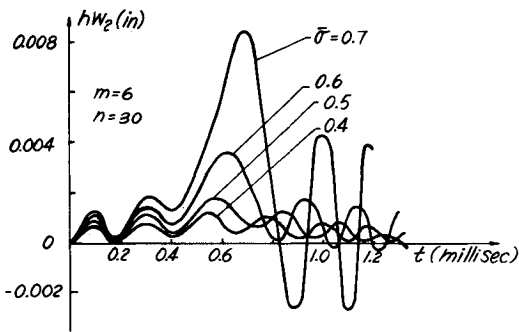


Fig. 8 Conical shell ( $\phi = 15^\circ$  and  $d_1 = 0.5$ ).

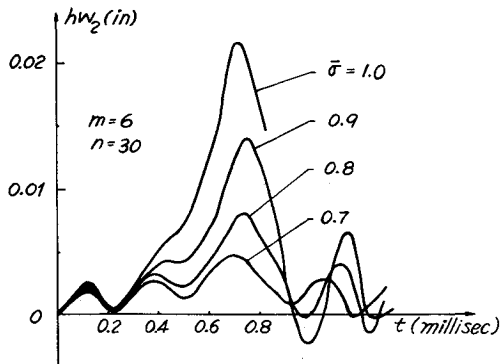


Fig. 9 Conical shell ( $\phi = 30^\circ$  and  $d_1 = 0$ ).

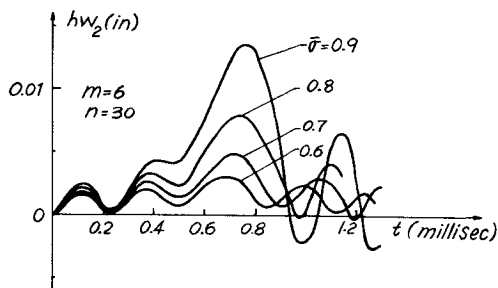


Fig. 10 Conical shell ( $\phi = 30^\circ$  and  $d_1 = 0.1$ ).

Table 1 Critical load  $\bar{\sigma}$  with several values of opening angle and initial imperfection

$d_1$	$\phi = 0^\circ$	$15^\circ$	$30^\circ$
0	0.6	0.65	0.95
0.1	0.45	0.6	0.9
0.5	0.4	0.55	0.9

functions may reflect unsuitable boundary conditions which can produce inconsistent stability results.

For example, a conical shell having an opening angle of  $90^\circ$  simply represents a flat circular ring. If the deformation functions and the initial imperfection are still chosen in the form of Eqs. (27) and (28), the ring clearly possesses no resistance to either transverse loads or in-plane compressions at the outer edge. A small movement in the transverse direction, i.e., the  $w$ -direction, for example, produces a rigid body motion.

Thus, it is necessary that the deformation functions be chosen so that they best approximate the shapes of the deflections and correctly describe the actual boundary conditions. Otherwise, the solution may correspond to that of a different problem. In fact, this is a central assumption imposed upon our approximation.

This example tends to suggest that Eqs. (27) and (28) not be used for opening angle greater than  $30^\circ$ . The established buckling load criterion also fails to determine the critical loads for the conical shells of large opening angles unless the deformation functions are properly modified.

D. Circular Rings

With appropriate modifications of the deformation functions, the cone analysis is applied to the ring problem. In this limiting case, however, the axial load becomes a transverse shear load distributed over the hole perimeter. Therefore, no dynamic

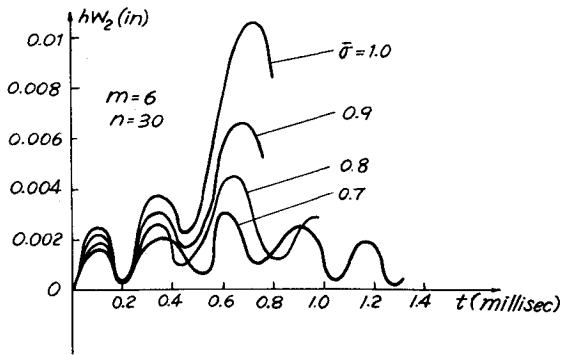


Fig. 11 Conical shell ( $\phi = 30^\circ$  and  $d_1 = 0.5$ ).

buckling is possible and numerical results indeed reflect this fact. Numerical results for both perfect and initially imperfect rings show that the time variation of the  $w_2$  mode exhibits oscillatory behavior and the buckling load criterion produces no critical load.

## V. Conclusions

In this analysis, a nonlinear shell theory has been employed to determine the dynamic response of a truncated thin circular conical shell structure which is loaded by an arbitrary time-dependent axial load and a uniform lateral hydrostatic pressure. The shell is permitted to have small initial imperfections.

A criterion for the dynamic buckling of a conical shell under a suddenly applied axial load is established. The two limiting cases, namely, the cylindrical shell and the flat circular ring, are examined along with the conical shell in this study.

The numerical results indicate that the axial load-carrying capacity of a cylindrical shell is greatly reduced by the presence of a small initial imperfection. The dynamic buckling load in this case agrees with results obtained by Roth and Klosner and Kempner. However, a conical shell structure is not as sensitive to its geometric imperfections as in the case of a cylindrical shell. The tendency of the dynamic instability of a conical shell structure decreases with the increase of the opening angle of the shell. The axial load-carrying capacity of a conical shell is found to be improved by an increase in its opening angle.

## References

- <sup>1</sup> Donnell, L. H., "A New Theory for the Buckling of Thin Cylindrical Shells under Axial Compression and Bending," *Transactions of the ASME*, Vol. 56, 1934, pp. 795-806.
- <sup>2</sup> Madsen, W. A. and Hoff, N. J., "The Snap-Through and Post-Buckling Equilibrium Behavior of Circular Cylindrical Shells under Axial Load," Sundaer 227, 1965, Dept. of Aeronautics and Astronautics, Stanford University, Stanford, Calif.
- <sup>3</sup> Almoth, B. O., "Influence of Imperfections and Edge Restraint on the Buckling of Axially Compressed Cylinders," Rept. 6-75-65-57, 1965, Lockheed Missiles and Space Co., Sunnyvale, Calif.; also AIAA-ASME Seventh Structures and Materials Conference, Cocoa Beach, Fla., 1966.
- <sup>4</sup> Koiter, W. T., "The Effect of Axisymmetric Imperfections on the Buckling of Cylindrical Shells under Axial Compression," *Proceedings of the Royal Netherlands Academy of Sciences*, Amsterdam, Ser. B, Vol. 66, 1963.
- <sup>5</sup> Roth, R. S. and Klosner, J. M., "Nonlinear Response of Cylindrical Shells Subjected to Dynamic Axial Loads," *AIAA Journal*, Vol. 2, No. 10, Oct. 1964, pp. 1788-1794.
- <sup>6</sup> Dym, C. L. and Hoff, N. J., "Perturbation Solutions of the Buckling Problems of Axially Compressed Thin Cylindrical Shells of Infinite or Finite Length," *Journal of Applied Mechanics*, Vol. 35, 1968, pp. 754-762.
- <sup>7</sup> Amazigo, J. C., "Buckling under Axial Compression of Long Cylindrical Shells with Random Axisymmetric Imperfections," *Quarterly of Applied Mathematics*, XXVI, 1969, pp. 537-566.
- <sup>8</sup> Van Slooten, R. A. and Soong, T. T., "Buckling of a Long, Axially Compressed, Thin Cylindrical Shell with Random Initial Imperfections," *Journal of Applied Mechanics*, Vol. 39, 1972, pp. 1066-1071.
- <sup>9</sup> Love, A. E. H., *A Treatise on the Mathematical Theory of Elasticity*, 4th ed., Dover Publications, New York, 1944, pp. 515-524.
- <sup>10</sup> Hoff, N. J., "Thin Circular Conical Shells under Arbitrary Loads," *Journal of Applied Mechanics*, Vol. 22, 1955, pp. 557-562.
- <sup>11</sup> Seide, P., "A Donnell Type Theory for Asymmetrical Bending and Buckling of Thin Conical Shells," *Journal of Applied Mechanics*, Vol. 24, 1957, pp. 547-552.
- <sup>12</sup> Budiansky, B. and Roth, R. S., "Axisymmetric Dynamic Buckling of Clamped Shallow Spherical Shells," *Collected Papers on Instability of Shell Structures*, TN D-1510, 1962, NASA.
- <sup>13</sup> Kempner, J., "Post Buckling Behavior of Axial Compressed Cylindrical Shells," *Journal of the Aeronautical Sciences*, Vol. 21, 1954, pp. 329-335.
- <sup>14</sup> Shiau, A. C., "Dynamic Buckling of a Truncated Conical Shell Structure," Ph.D. Dissertation, Sept. 1973, State University of New York at Buffalo, Buffalo, N.Y.